Chimeric Liquid Crystallinity: Noncovalent Association of DNA and Bacterial Levan

Anne E. Huber[†] and Christopher Viney*[,‡]

Center for Bioengineering, Box 357962, University of Washington, Seattle, Washington 98195, and Department of Materials, University of Oxford, Parks Road, Oxford OX1 3PH, U.K.

Received November 19, 1996; Revised Manuscript Received February 17, 1997[⊗]

ABSTRACT: The liquid-crystalline phase of cell-free and nominally pure bacterial levan in water is shown to depend on the presence of DNA. The necessary concentrations of DNA are 2 orders of magnitude lower than those needed to stabilize a mesophase in aqueous solutions of DNA on its own and are similarly small in comparison to the number concentration of the globular levan molecules. A partial phase diagram for liquid crystallinity in the ternary system water/levan/DNA is mapped out. A model is proposed in which the levan and DNA associate noncovalently, to produce supramolecular, rodlike aggregates. The term "chimeric liquid crystal" is coined to denote a mesophase based on such rods assembled from otherwise unrelated molecular species. The model can account for several characteristics of the liquid-crystalline phase of bacterial levan, including the unexpected observation that liquid crystal phase formation is accompanied by a continuous increase in viscosity.

Introduction

Levan is a branched biopolymer assembled from D-fructose monomers. β (2 → 6) linkages occur along the main chain and within side chains, and branches are attached to the main chain through β (2 → 1) linkages (Figure 1). The molecular weight and degree of branching depend on the levan source. Low molecular weight levan with minimal branching can be found in grasses;[1,2] in contrast, levan produced by bacteria is characterized by a high molecular weight[3] which may exceed 10^7, and there are side chains on up to 30% of the main-chain residues.[4] Large-scale production of levan and regulation of the purity and molecular weight are achievable by controlled bacterial synthesis. The high molecular weight bacterial levans are being considered for a variety of applications that include biodegradable food packaging and coatings.[2,5]

Both materials processability and the control of molecular alignment are important issues in the manufacture of packaging. The liquid-crystalline state (either solution or melt) offers several well-documented advantages in both of these respects.[6−8] It has been demonstrated[9,10] that aqueous solutions of cell-free and nominally pure bacterial levan[3] are able to form a nematic liquid-crystalline phase at low concentrations and at ambient temperatures (Figure 2). Subsequent research has revealed how the addition of starch, a nonmesogenic filler, affects the stability of the nematic phase.[11]

The phase diagrams for these systems were determined by turbidity measurements made with a UV−visible spectrophotometer.[10−12] Solution absorbance spectra show a large peak centered at around 260 nm (Figure 3); it is assignable to electronic transitions that are characteristic of the aromatic groups found in nucleic acid impurities.[13] Since the levan molecule does not itself contain such groups, the large 260 nm peak should not be present in a molecularly pure sample. The preparation of levan from bacterial cells[3,14] implicates a possible source of both DNA and RNA. Even though the levan had been subjected to several purification steps,[3] the procedures used do not preclude a residual presence of bound nucleic acid in the levan powder. In this paper, we describe the methods that we used to identify and remove the bound impurities. We then present evidence that the "rods" responsible for the liquid crystallinity in aqueous solutions of bacterial levan are not polysaccharide molecules with an extended conformation but linear aggregates of globular levan formed around cores of residual DNA.

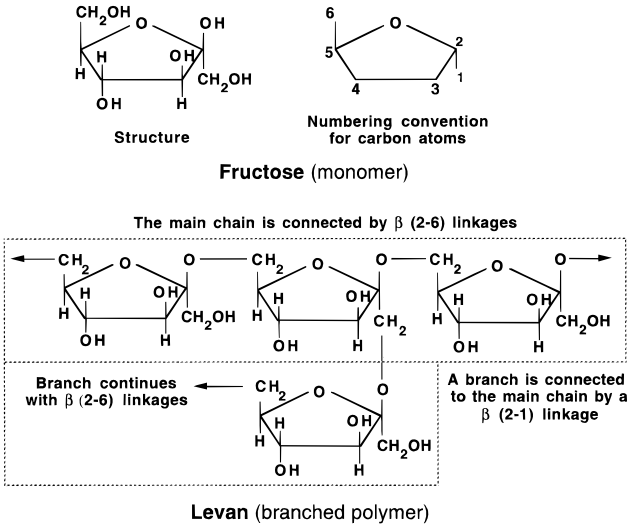

Figure 1. Schematic representation of a branched levan chain and its fructose monomer.

Materials and Methods

Removal of Nucleic Acid Impurities. (a) Gel Electrophoresis. Gel electrophoresis was used to identify the type (RNA or DNA) and approximate molecular weight of the nucleic acid impurities.

Cell-free levan powder, synthesized by *Bacillus polymyxa* bacteria,[3] was obtained from the U.S. Army RD&E Center, Natick, MA. A 5 wt % aqueous solution was prepared.

RNAse (Sigma Chemical Co., RNAse A Type 1-AS) was prepared at a concentration of 10 mg/mL in 0.01 M sodium acetate, followed by heating to 100 °C for 15 min, adjusting pH to 7.4 with Tris-HCl, and storage at −20 °C. This protocol ensures that the RNAse is free from contamination by DNAse.

* Author to whom correspondence should be addressed.
† University of Washington.
‡ University of Oxford.
⊗ Abstract published in *Advance ACS Abstracts,* April 1, 1997.

S0024-9297(96)01705-6 CCC: $14.00

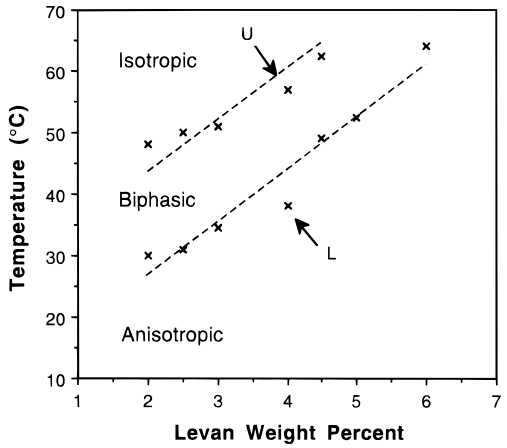

Figure 2. Partial phase diagram for dilute aqueous solutions of cell-free and nominally pure levan. The diagram differs in slight detail from that published previously,[10] due to automation of the data collection method.[12] The representative points U and L are determined from turbidity measurements and correspond to points U and L in Figure 4.

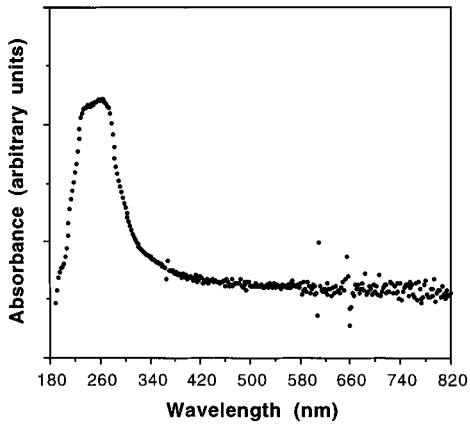

Figure 3. Typical absorption spectrum (raw turbidity data) acquired with the UV-visible spectrophotometer. The specimen was a 4 wt % solution of as-received levan at 20 °C.

DNAse (Boehringer Mannheim, DNAse 1 grade 1) was prepared at 10 mg/mL in a 1 mM MgCl solution.

A total of 10 μL of the levan solution was mixed either with excess RNAse (2 μL) or with excess DNAse (2 μL) and incubated at 37 °C for 30 min. A total of 2 μL tracking dye containing bromophenol blue, xylene cyanol FF, glycerol, and water was added before samples were loaded on the gel. A third lane was loaded with 10 μL of the levan solution mixed with 2 μL of the tracking dye only.

A standard molecular weight marker was prepared by mixing 5 μL of Lambda Hind III ladder (Gibco BRL) with 5 μL of ddH_2O and 2 μL of tracking dye.

Electrophoresis was performed on a 1 wt % agarose gel prepared in TAE (40 mM Tris-acetic acid−1 mM EDTA) buffer. The gel was poured in an 8.5 × 20.4 cm form, was run at 86 V for 2 h to obtain a straight dye front, and was stained in ethidium bromide.

(b) Ion-Exchange Chromatography. Following identification of the nucleic acid impurities, the as-received levan was purified by ion-exchange chromatography. A Bio-Rad Macro-Prep DEAE ((diethylamino)ethyl—a weak anion-exchange group with a pH stability in the range of 1−14) support was chosen. Both RNA and DNA possess a net negative charge, while levan carries zero net charge; therefore, levan is able to travel through the matrix without binding. Distilled deionized water was used as the eluent because levan is water soluble and also because this choice obviates the need to subsequently remove salt from the eluted levan solution.

Two sizes of columns were used: (1) Solubilized levan was passed repeatedly over a short column (8 cm length, 2.5 cm diameter) to obtain material of decreasing impurity content. (2) On the basis of impurity characterization performed on these samples, material used in all subsequent studies was purified by passing solubilized as-received polymer through a long column (32 cm length, 2.5 cm diameter).

Columns were poured and then washed with two bed volumes of a 1.5 M NaCl aqueous solution. The salt was removed with a wash of two bed volumes of ddH_2O. A 10 mL aqueous solution containing 2 wt % as-received bacterial levan was equilibrated on a rotator for at least 2 h to allow all of the powder to go into solution. The solution was then loaded onto the column, using ddH_2O as the eluent. Purified levan exited the column with the eluent and was lyophilized into a powder. The nucleic acids were then eluted from the column with two bed volumes of 1.5 M NaCl to restore the column for re-use.

Lyophilization of the purified levan was accomplished with a UNI-TRAP lyophilizer Model 10-100 (Vitris Co.). Light scattering (see below) verified that the levan was intact. Due to slight differences in their purity, the batches of levan run through the column were combined to provide a homogeneous stock of powder for subsequent experiments.

Levan purified on the 32 cm column still contained detectable nucleic acid levels, as revealed by gel electrophoresis and nucleic acid molecular probes. However, turbidity measurements made with a UV−visible spectrophotometer were no longer able to detect liquid-crystalline transitions in aqueous solutions of this levan.

(c) Fluorescence Assays. The removal of nucleic acids was monitored both by gel electrophoresis (as described above) and with a nucleic acid molecular probe. YO-PRO (YO-PRO 1 in DMSO) from Molecular Probes, Eugene, OR, was used. It is a monomeric probe whose fluorescence is almost zero when unbound, and it possesses good photostability when fluorescing. The binding affinity to double-stranded DNA is very high, and slightly lower for RNA and single-stranded DNA.[15] YO-PRO was purchased at 1 mM concentration in 1 mM DMSO. Standard fluorescence curves were prepared using ctDNA (Sigma Chemical Co., calf thymus DNA, activated) and tRNA (Sigma Chemical Co., transfer RNA, type X-SA), which were chosen for having molecular weights similar to those of the nucleic acid impurities found in levan. Samples from 0 to 10 000 ng (nucleic acid)/mL (H_2O/YO-PRO solution) were prepared with a final volume of 500 μL and a YO-PRO concentration of 2 μM. Aqueous levan samples at 0.5 wt % levan were prepared from as-received levan, and from levan that had been run over the short (8 cm) column either once, twice, or three times. H_2O/YO-PRO was added to these samples to obtain a final volume of 500 μL and a YO-PRO concentration of 2 μM, and the samples were then characterized by fluorescence spectroscopy. The samples were excited at 485 nm on a Hitachi Model F-4500 fluorescence spectrophotometer, and an emission spectrum was collected from 450 to 600 nm. Data points at 530 nm were used for comparison and plotting. Both the excitation and emission slit widths were set at 5 nm, and the scan speed for all measurements was 240 nm/min. The standard nucleic acid curves were used to estimate the amount of nucleic acid impurity present in levan following various degrees of purification.

(d) Dynamic Light Scattering. Dynamic light scattering was used to verify that the levan molecules were not damaged by the ion-exchange column or by lyophilization. A dynamic laser light scattering system, comprised of a Spectra Physics Stabilite HeNe laser Model No. 124A and a Pacific Instruments photomultiplier tube detector, was aligned for use. The laser was set at a 20° apparent angle for the measurements. Solutions of as-received levan and purified levan at 2.5 mg/mL were prepared in ddH_2O with 0.1 wt % sodium azide added to combat microorganism growth. Measurements were taken over time scales ranging from 40 to 200 ms. In order to enable a direct comparison between the purified and unpurified levan solutions, it was necessary to add microspheres (4.26 μm diameter) to the purified sample to eliminate homodyning.[16]

Addition of Nucleic Acids. We found that the liquid-crystalline phase transitions exhibited by solutions of as-received levan were eliminated by purification, and therefore

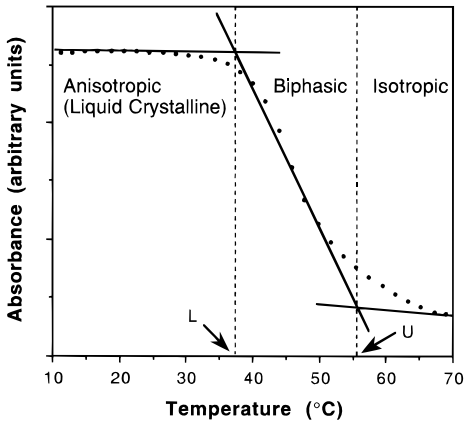

Figure 4. Illustration of how a plot of absorbance versus temperature provides information for constructing a phase diagram. The data were obtained from a 4 wt % aqueous solution of as-received levan. L and U identify the lower and upper limits of the temperature range in which the sample turbidity changes most rapidly (due to a continuously changing volume fraction of liquid-crystalline material in the sample). These limits define the correspondingly labeled points in Figure 2.

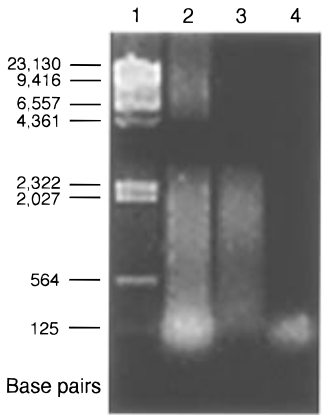

Figure 5. Agarose gel showing the presence of nucleic acid impurities in as-received levan. Lane 1: molecular weight marker. Lane 2: as-received levan. Lane 3: as-received levan plus RNAse. Lane 4: as-received levan plus DNAse.

we studied the effect of selectively adding back molecular species similar to those that had been removed.

Since RNA represented a large percentage of the nucleic acid impurities, 40 μg of transfer RNA (an amount close to the impurity concentration in as-received levan as estimated from the Nucleic Acid Molecular Probe experiments) was added to a 5 wt % solution of purified levan. Transfer RNA (Sigma Chemical Co., transfer RNA, type X-SA) was chosen: it is a common type of RNA, and it has a molecular weight approximately equal to that of the RNA impurities found in the levan and quantified by gel electrophoresis.

Because tRNA did not restore liquid crystallinity in solutions of the purified levan, we prepared solutions of purified levan containing various concentrations of added DNA. Solutions were prepared at levan concentrations ranging from 1 to 7 wt %, containing ctDNA additions of 0.002 to 0.017 wt %. Calf thymus DNA was used, for two reasons. First, it has a molecular weight profile similar to that of DNA impurities that were removed from the levan. Second, ctDNA can be obtained readily in the relatively large quantities necessary for these experiments.

Characterization of Liquid Crystallinity. (a) Transmitted Polarized Light Microscopy (TPLM). It was necessary to reassess the liquid crystallinity of aqueous solutions following purification of the levan. Aqueous solutions containing from 1 to 8 wt % purified levan were examined using TPLM, as done previously[10] for solutions of the as-received polymer. Samples for microscopy were prepared from each solution by transferring 10 μL aliquots of the fluid to glass slides (precleaned Gold Seal Micro Slides, A-1450, Clay-Adams Division, Becton Dickinson, used as-received). Two samples were prepared at each concentration: one with a cover slip (Corning No. 1 cover glass, Corning Glass Works, used as-received) and one without. Samples were observed intermittently by TPLM over several days.

TPLM was used similarly to characterize the water/purified levan/tRNA and water/purified levan/ctDNA specimens. Sodium azide was present at 0.1 wt % in all samples, to combat microorganism growth.

(b) Turbidity Measurements. Turbidity measurements were used in earlier experiments to determine the liquid-crystalline phase boundaries for solutions of as-received levan; the technique has been described in detail elsewhere.[10,12] A typical raw sample scan is shown in Figure 3. Data at 700 nm were plotted as a function of temperature, as illustrated in Figure 4. Rapid changes of slope on such plots were used to construct the phase diagram (Figure 2).

In the present studies, turbidity measurements were performed on solutions of purified levan, in the concentration range 1−7 wt % levan and from 10 to 70 °C. The water/purified levan/tRNA and water/purified levan/ctDNA specimens described above were characterized over the same temperature range. Sodium azide was present at 0.1 wt % in all samples, to combat microorganism growth.

(c) Viscosity Measurements. Liquid crystallinity in polymer solutions is conventionally associated with low viscosity, with useful consequences for processing. Viscosity measurements were performed with a falling ball viscometer,[17] designed for use on small volumes (approximately 100 μL) of dilute solutions at room temperature (approximately 20 °C). The capillary tube was inclined at 30°, measured from horizontal. Experiments were performed on solutions of as-received levan at concentrations from 1 to 6 wt %, and on solutions containing 4 wt % purified levan and 0.0, 0.002, 0.004, 0.007, 0.010, 0.014, or 0.017 wt % ctDNA. Two samples of each composition were prepared; five measurements were made on each sample, with approximately 2 min elapsing between measurements.

Results and Discussion

Removal of Nucleic Acid Impurities. (a) Gel Electrophoresis. The agarose gel shown in Figure 5 demonstrates that nucleic acid impurities are present in the as-received levan. Lane 2 shows that the impurities are spread over the whole molecular weight range examined (see molecular weight markers in lane 1). There is also a dense band centered slightly below 125 bp. Lanes 3 and 4 indicate that the dense band arises from RNA content in the as-received levan, while the highly polydisperse impurity is a combination of RNA and DNA. In a control sample treated with both DNAse and RNAse, the nucleic acid content was reduced to an undetectable level (data not shown).

(b) Ion-Exchange Chromatography and Fluorescence Assays. After identification of both RNA and DNA impurities, ion-exchange chromatography was used to remove the nucleic acids while preserving the levan molecules intact. Figure 6 shows the decrease in nucleic acid content with successive passes over the 8 cm Bio-Rad Macro-Prep DEAE ion-exchange column. The majority of the nucleic acids were removed, as determined both by nucleic acid molecular probes and by gel electrophoresis (Figure 7).

(c) Dynamic Light Scattering. Figure 8 shows spectra for as-received levan, purified levan, and purified levan with microspheres added. The time constant obtained from the purified levan is approximately half that obtained from the as-received levan; this homodyning effect[16,18] suggests that purification has either (1) removed large impurities or (2) destroyed structures

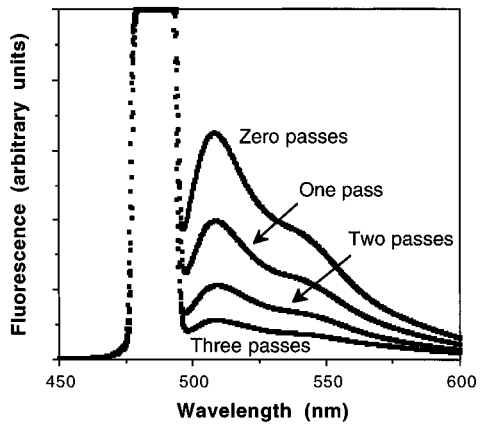

Figure 6. Progression of nucleic acid removal with successive passes over an 8 cm DEAE column.

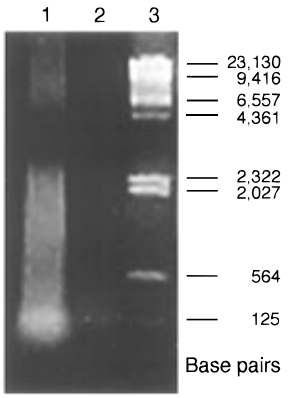

Figure 7. Agarose gel comparing as-received and purified levan. Lane 1: as-received levan. Lane 2: levan after purification on a 32 cm ion-exchange column. Lane 3: molecular weight marker.

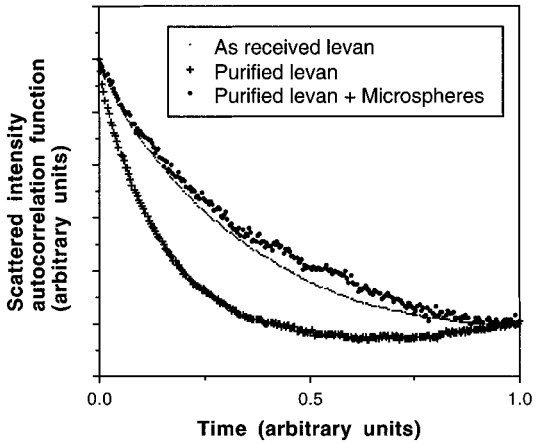

Figure 8. Comparison of dynamic light scattering data for as-received levan, purified levan, and purified levan with 4.26 μm diameter microspheres added.

that are large in comparison to the levan molecules recovered after purification.

Addition of the microspheres leads to a spectrum comparable to that obtained from as-received levan. The most simple interpretation of this result is that the molecular weight distribution of the levan has not been changed significantly by purification (i.e., its characteristics are the same in all three samples), and that the solutions of as-received levan contain impurities or aggregates with a linear dimension similar to the size of the microspheres.

Phase Behavior of Purified Levan in Aqueous Solution. (a) Transmitted Polarized Light Microscopy. Microscopic examination of the solutions prepared from purified levan revealed no evidence of liquid-crystalline order. Either the ability of molecules to form sufficiently anisotropic structures has been eliminated by the purification or the domain size is now too small to be resolved by this technique.

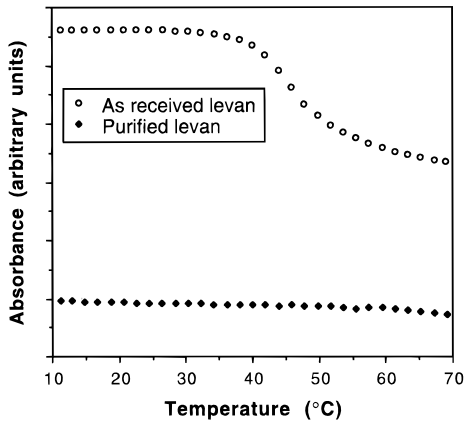

Figure 9. Comparison of the turbidity profiles for 4 wt % aqueous solutions of as-received and purified levan.

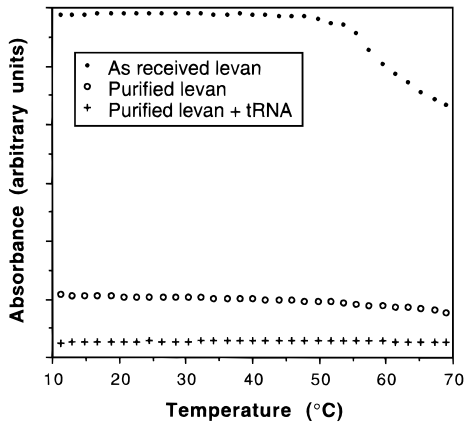

Figure 10. Absorbance data comparison for as-received levan, purified levan, and purified levan with tRNA added. The levan solutions were prepared at 5 wt % in each case; baseline turbidities are therefore higher than those in Figure 9.

(b) Turbidity Measurements. Figure 9 demonstrates the change in turbidity between the as-received levan and the purified levan at 4 wt %, in the temperature range 10−70 °C. The baseline turbidity of the purified sample is lower, and the phase transitions noted in Figure 4 are not present in the sample prepared from purified levan. Similar observations were made at all of the concentrations examined, providing the initial evidence that one of the nucleic acid impurities is necessary for liquid-crystalline order to develop in aqueous levan solutions.

Addition of Nucleic Acids. (a) Turbidity Measurements. As can be seen in Figure 10, addition of tRNA to the purified levan had little effect. This is unremarkable, since tRNA is not rodlike in shape,[13] and is not itself known to form liquid-crystalline solutions. Rodlike moieties are needed to stabilize nematic order.[19]

Figure 11 demonstrates how additions of ctDNA affect aqueous solutions of purified levan. Liquid-crystalline transitions, similar to those seen previously in solutions of as-received levan, occur in several of the water/purified levan/ctDNA samples. It therefore became appropriate to compile the phase transitions into a ternary phase diagram. Conventionally, the diagram would be referred to triangular coordinates, with the

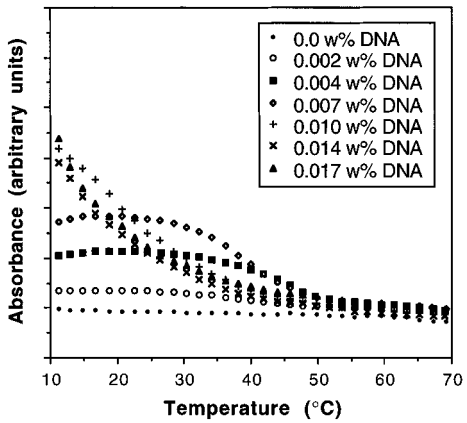

Figure 11. Absorbance data for purified levan (4 wt % solution) with ctDNA added.

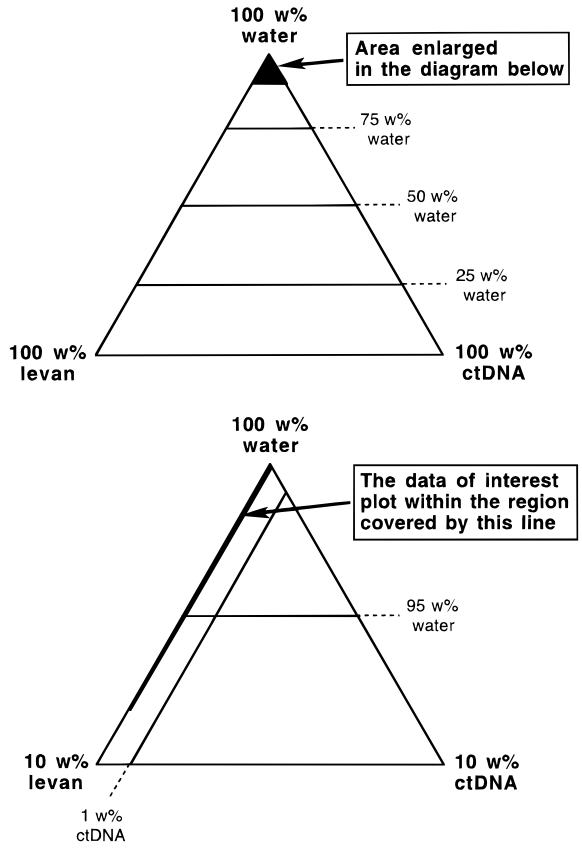

Figure 12. Schematic ternary phase diagram of water/purified levan/ctDNA, using conventional triangular coordinates.

three components plotted at the corners of an equilateral triangle.[20] However, our solutions are dilute with respect to levan and especially ctDNA, so that the region of interest would not be usefully resolved on such a diagram (Figure 12). We therefore resorted to an older but now little-used method of plotting phase diagrams for three-component systems.[21]

A plot is made on Cartesian axes for each temperature of interest. The units plotted along the two axes are [amount of component B/amount of component A] and [amount of component C/amount of component A]. Component A is the material present in the largest concentration, in this case water. Data such as those shown in Figure 11 are used to determine whether the sample is in the isotropic, heterogeneous, or anisotropic phase at specific combinations of temperature and concentration. Figure 13 shows the phase diagram for

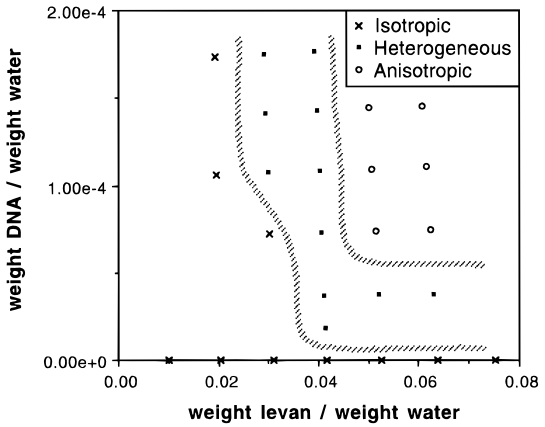

Figure 13. Partial phase diagram for water/purified levan/ctDNA at 10 °C. Phase boundaries are indicated approximately. In a system containing more than two components, compositions that phase-separate are not restricted to forming just two phases; the term "heterogeneous" (rather than "biphasic") is therefore used to denote the phase-separating compositions.

water/purified levan/ctDNA at 10 °C. Similar plots were constructed at every 10 °C from 20 to 70 °C (Figure 14).

(b) Transmitted Polarized Light Microscopy. The turbidity measurements were corroborated by TPLM. No detectable liquid-crystalline textures formed in the water/purified levan/tRNA solutions. In contrast, water/purified levan/ctDNA samples that lie in the liquid-crystalline region of the phase diagram at room temperature exhibited nematic liquid-crystalline textures similar to those seen in solutions of as-received levan.[9,10]

(c) Viscosity. It is convenient to address the viscosity data for both water/as-received levan and water/purified levan/ctDNA in a single section.

The results of measurements performed on solutions of as-received levan are shown in Figure 15. There are two significant features of this plot. First, there is more scatter in the data at higher solution concentrations. For the 4, 5, and 6 wt % solutions, successive measurements on the same sample distinguishably yielded increasing viscosity values, as is shown explicitly for the two 6 wt % specimens in Figure 15. This trend is in the opposite direction to what would be expected if molecular weight degradation were occurring. Second, the average value of viscosity increases monotonically and rapidly with increasing concentration of the liquid-crystalline phase. This behavior runs contrary to the conventional wisdom that viscosity of a lyotropic system should peak at concentrations within the heterogeneous regime;[8,22,23] in other words, the single-phase anisotropic solution would normally have a viscosity comparable to that of the single-phase isotropic solution. A molecular model that is consistent with this unexpected effect is offered below.

From the 20 °C data in Figure 11, it is seen that solutions containing 4 wt % purified levan plus 0.002, 0.004, 0.007, 0.010, 0.014, or 0.017 wt % added ctDNA fall within the heterogeneous region of the phase diagram. Figure 16 presents the results of viscosity measurements performed on these samples. The data show a marked, continuous increase in solution viscosity with the addition of ctDNA. Again, therefore, there is no evidence of a viscosity maximum in the heterogeneous regime.

A comparison of Figures 15 and 16 reveals that purifying the levan leads to a marked reduction in the

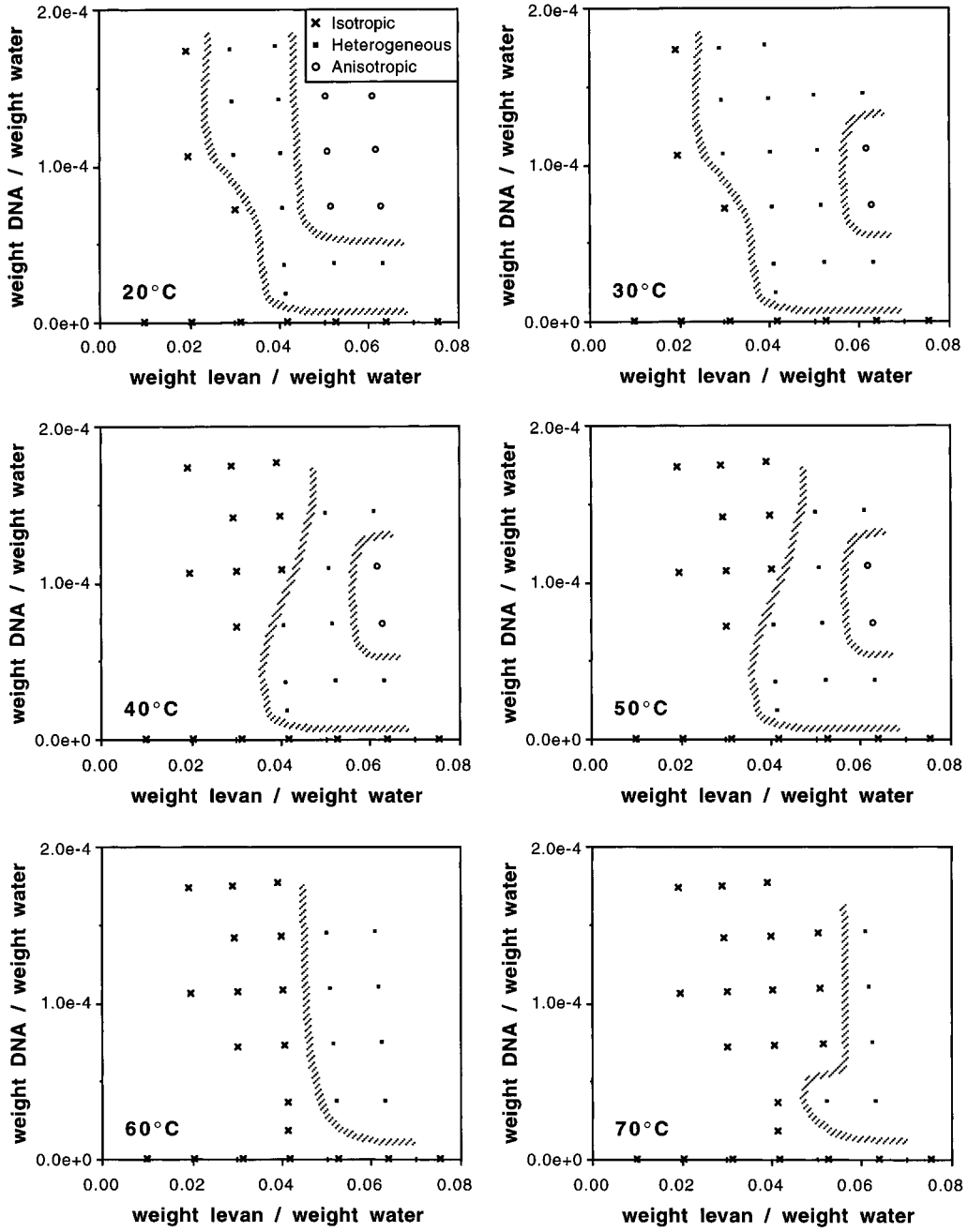

Figure 14. Partial phase diagram for water/purified levan/ctDNA at 10 °C intervals in the range 20−70 °C. Phase boundaries are indicated approximately.

solution viscosity, regardless of whether or not ctDNA has been added subsequently. This result suggests that RNA makes a significant contribution to the viscosity of solutions prepared from as-received levan. The three-dimensional shape of tRNA resembles a "hand-held drill",[13] which would promote a higher solution viscosity. Also, given the tendency of RNA to copurify with levan and DNA (evident from its presence in the as-received material), it is possible that RNA promotes aggregation within the solutions.

Molecular Model. A molecular model for solutions of bacterial levan must accommodate all of the following facts:

(1) Solutions of purified levan do not form detectable liquid-crystalline phases, in contrast to solutions of as-received levan.

(2) Solutions of purified levan are significantly less turbid than solutions prepared from as-received levan.

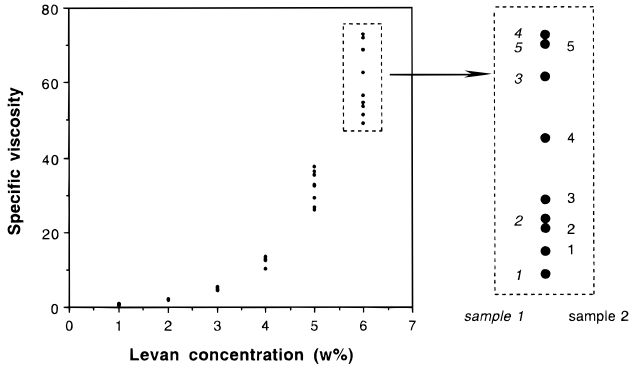

Figure 15. Viscosity measurements for as-received levan at increasing concentration in water. Sets of five successive measurements on each of two 6 wt % samples are also shown.

(3) Light scattering indicates that structures with a linear dimension of a few micrometers are present in

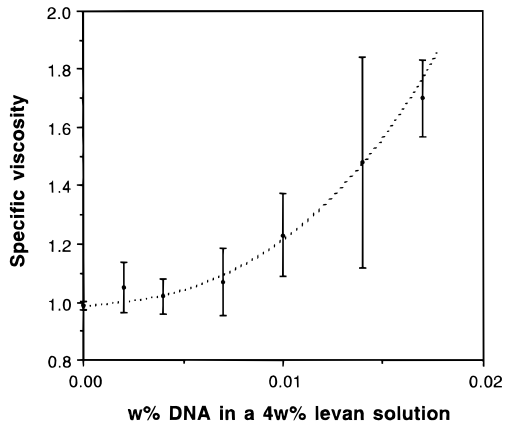

Figure 16. Viscosity measurements for 4 wt % solutions of purified levan with varying amounts of ctDNA added.

isotropic aqueous solutions of as-received levan but not purified levan.

(4) Levan molecules in solution have been shown experimentally to adopt compact, spherically symmetrical, globular conformations.[24] The globular molecules do not interact with *each other* to form aggregates.[24] Modeling studies that predict a left-handed helical conformation for the molecules[25] are less definitive than the experimental work, because the models consider only short molecular fragments and do not take branching into account.

(5) Aqueous levan solutions form a liquid-crystalline phase if DNA is present. The necessary concentrations of DNA are 2−3 orders of magnitude lower (by weight) than the concentration of levan. They are also approximately 3 orders of magnitude lower than the critical concentration for lyotropic behavior in solutions of pure DNA of comparable molecular weight. In our experiments, the "typical" DNA molecule (7.6×10^6, the estimated midpoint of the relevant band obtained in gel electrophoresis) is ∼4 μm long and promotes liquid crystallinity at concentrations as low as ∼0.07 mg/mL. (The conversion from molecular weight to length is achieved by noting that the weight of a single base pair in DNA is 650, there are 10 base pairs in one repeat of the double helix, and the length of the helix repeat is 34 Å.[26]) In the absence of levan, aqueous solutions of DNA molecules that are ∼3 μm long do not form a mesophase until a concentration of ∼13 mg/mL is exceeded.[27]

Scaled in terms of the relative number of molecules, liquid-crystalline solutions of composition 4 wt % levan and 0.007 wt % ctDNA contain approximately 183 levan molecules for every molecule of DNA. This estimate uses the "typical" DNA molecular weight given above and a "typical" levan molecular weight of 2.3×10^7 (the midpoint of the measured molecular weight range[3]).

(6) The axial (length-to-width) ratio of the rods that align in the liquid-crystalline phase of water/levan/DNA is a decreasing function of temperature.[10,12] This is reflected in the finite, positive gradient of the phase boundaries in Figure 2.

(7) The evolution of liquid-crystalline order in water/levan/DNA solutions is accompanied by a continuous increase in viscosity.

(a) Aggregates. These observations collectively and consistently suggest that levan and DNA molecules can interact to form rodlike aggregates, which, if present in sufficient concentration, can then become aligned in the liquid-crystalline phase. DNA contributes geometrical anisotropy to the aggregates, while bound levan helps to raise the volume fraction of the rods above the critical value needed to stabilize liquid-crystalline order.

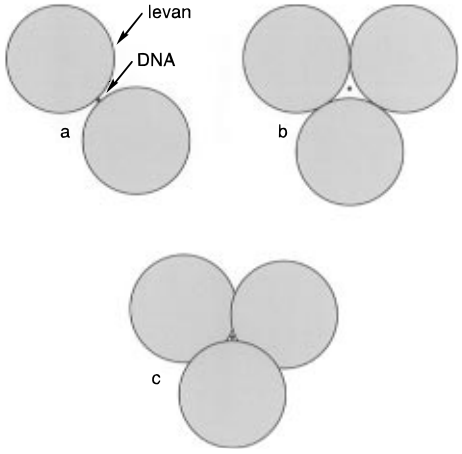

Figure 17. Simple packing schemes of spherical levan molecules around a cylindrical (rodlike) DNA core. The diameters of DNA and a typical levan molecule are shown approximately to scale.

Aggregation of globular biopolymer molecules into rodlike structures capable of forming liquid-crystalline phases has been recognized in several contexts. Examples include the assembly of F-actin from G-actin,[28,29] microtubules from tubulin,[30] Hemoglobin-S,[31] and silk.[32,33] The novel aspect of the levan/DNA aggregates proposed here is that they incorporate two otherwise unrelated types of molecules. For this reason, we use the term "chimeric liquid crystal" to refer to the mesophase formed by the aggregates at sufficiently high concentration. The type of interaction responsible for levan/DNA binding has yet to be determined. However, the existence and effectiveness of such binding is demonstrated by the difficulty of purifying the levan.

In the following sections, some characteristics of the proposed aggregates are derived, and their consequences are discussed in terms of the experimental data.

(b) Levan:DNA Ratio in Aggregates. As noted above, the "typical" added ctDNA molecule is approximately 40 000 Å long. The diameter of double-helical DNA is approximately 20Å.[26] In aqueous solutions of levan having a molecular weight distribution comparable to that of our material, the "typical" molecule has a radius of gyration of ∼350 Å at 25 °C,[24] i.e., an effective diameter of 700 Å.

Figure 17a schematically shows levan molecules packed in a simple 2-fold configuration around a DNA core. On the basis of the typical dimensions given above, 114 levan molecules could associate with each DNA core in this arrangement. Figure 17b shows a simple 3-fold configuration of levan around DNA. In this case, there can be as many as 171 globular levan coils around each DNA rod. The central "hole" in Figure 17b can, in fact, accommodate a cylinder of up to 108 Å diameter, or 88 Å larger than is necessary to fit the DNA (the critical radius ratio of the hole relative to the surrounding levans in this configuration is $2/\sqrt{3} - 1$). Given that the levan coils are flexible, it might be thought possible for them to distort so as to obtain a close contact with the DNA. However, the necessary distortion is a nontrivial fraction of the levan coil radius; for a molecule that favors a randomized conformation, the entropy penalty of such a distortion can be expected to outweigh the enthalpic benefits of binding to another molecule.[34] A more likely refinement is that the levan

molecules pack densely in a spiral fashion around the DNA core (one possibility is shown in Figure 17c), implying a levan-to-DNA binding ratio between 114 and 171. This rough prediction is of comparable magnitude to the experimentally estimated value of 183 noted above. A further refinement of the model would incorporate the polydispersity of the levan.

The simple model, therefore, provides a basis for understanding how the molecular order of levan in water can be influenced significantly by comparatively small amounts of DNA. A closer match between the estimated numbers obtained from the model and from experiment is not expected, for several reasons. First, the purified levan is still not DNA-free. Second, our experiments have not identified the *minimum* amount of DNA needed to stabilize liquid crystallinity in a solution of given levan concentration. Third, the development of liquid-crystalline order need not require all the levan to be bound to DNA. Finally, the polydispersities of the levan and DNA have not been incorporated in the geometric description of the model, and the assignment of "typical" values of molecular weight was done approximately.

(c) Axial Ratio of Aggregates Decreases as Temperature Increases. The boundaries in the phase diagram for water/as-received levan (Figure 2) have a positive slope. Interpreted simply, this observation suggests that the axial ratio of the rods constituting the liquid-crystalline phase becomes smaller as the temperature is raised.[35] Previously, before recognizing the role played by DNA in this liquid-crystalline phase, we attempted to interpret the axial ratio change in terms of changes in the persistence length of extended levan conformations.[10]

From the dimensions of levan and DNA given above, the diameter of a representative levan/DNA aggregate can be estimated as follows:

$$\text{aggregate diameter} = (2 \times \text{"typical" levan diameter}) + \text{DNA diameter}$$

$$= (2 \times 700\ \text{Å}) + 20\ \text{Å} \quad \text{at } 25\ ^\circ\text{C}$$

$$= 1420\ \text{Å}$$

Therefore, the approximate axial ratio is (length of a "typical" DNA molecule)/(diameter of an aggregate) = $(4 \times 10^4)/1420 \approx 28$ for a "typical" aggregate. This value lies above the critical axial ratio of ≈6 that several models predict as necessary for rodlike moieties to self-assemble into a liquid-crystalline phase.[36]

As temperature is increased, the levan coils expand. Stivala indicates that the radius of gyration increases to 41 nm at 57 °C.[24] Therefore, the diameter of the "typical" aggregate has increased:

$$\text{aggregate diameter} = (2 \times 820\ \text{Å}) + 20\ \text{Å} = 1660\ \text{Å} \quad \text{at } 57\ ^\circ\text{C}$$

The new axial ratio is $(4 \times 10^4)/1660 \approx 24$ (assuming that the DNA length has not changed significantly). Therefore, axial ratio decreases with temperature increase.

If we assume that the interactions between aggregates are "hard", the critical rod volume fraction V^* required to stabilize liquid-crystalline order can be estimated from Flory's equation:

$$V^* \approx \frac{8}{x}\left(1 - \frac{2}{x}\right)$$

where x denotes the rod axial ratio.[37,38] Substituting the values of x as estimated above, we predict that V^* increases by approximately 0.04 on heating from 25 to 57 °C. However, increasing the temperature also causes the aggregate volume fraction to increase, without any more aggregates being added to the solution, because the diameter of the aggregates increases as the levan coils expand. One must, therefore, ask whether this increase in volume fraction, at constant composition by weight, could be sufficient to maintain liquid crystallinity—in other words, can it provide the increase in volume fraction required to compensate for the effect of the decreased axial ratio? Given the aggregate geometry described above, together with values for the density of water [39] (997.0 kg·m^{-3}) at 25 °C and 984.7 kg·m^{-3} at 57 °C), it is easily shown that the necessary volume fraction increase of 0.04 would require an initial volume fraction of at least 0.13. Therefore, in more dilute solutions, additional aggregates must be introduced to preserve stable liquid crystallinity if a sample initially at the critical concentration is heated. This is consistent with the positive slope of the boundary between the isotropic and biphasic fields recorded in Figure 2. The upper limit of the concentration range in Figure 2 is dictated by sample viscosity: it is not possible to prepare homogeneous samples or to perform reliable characterization of liquid crystallinity at concentrations above 10 wt %.

Finally, we note that the increase in the radius of levan coils on heating means that fewer can be accommodated in a single aggregate (it will not be possible to pack as many around a DNA molecule); the free levan will disrupt the ability of the aggregates to align. More aggregates per unit volume will, therefore, be needed to compensate for this and stabilize liquid-crystalline order.

(d) Viscosity. Figure 15 shows that solution viscosity for as-received levan increases monotonically as concentration increases. In the isotropic state, the viscosity−concentration dependence simply reflects the increased chance of aggregate interaction at higher concentrations. The fact that the viscosity continues to increase as concentration rises above the critical value for single-phase liquid crystal formation can be assigned to three factors. First, the levan is polydisperse, so the aggregates would not have the simple cylindrical or lathlike geometry conventionally associated with the rods in a nematic or cholesteric liquid crystal. The aggregates would necessarily have a rough profile, which precludes an ability to slide past each other easily, even though they can align. Second, because the aggregates consist of noncovalently bonded species, it is expected that levan can be dislodged during shear, enhancing further the surface topography of the aggregates. Successive measurements made on a given sample at short time intervals ought therefore to detect an increase in viscosity that is especially marked in more concentrated samples, as is observed. (This same observation leads us to discount possible incidences of single levan molecules binding to *two or more* DNA molecules. Such cross-links would be especially sensitive to shear. Were they initially present in any significant concentration, successive viscosity measurements on a given sample should tend toward a lower, not higher, value of viscosity.) Third, even though the overall *proportion* of levan to DNA remains constant as the concentration of as-received "levan" increases, the concentration of any unassociated levan dispersed in the

solvent can increase, also promoting a rise in viscosity.

Adding ctDNA to a solution of purified levan (Figure 16) will enable aggregate formation, leading to increased molecular interaction and increased viscosity. Again, the aggregate geometry must reflect the polydispersity of the levan, precluding easy relative displacement and conventional (low-viscosity) liquid-crystalline behavior.

Acknowledgment. We gratefully acknowledge tutorial conversations with Drs. Patrick Stayton, Fred Gittes, David Kaplan, and Lisa Gilliland (who proposed the designation "chimeric" liquid crystal) and with Cyndi Long. Alfred Allen (U.S. Army RD&E Center, Natick, MA) kindly provided samples of bacterial levan. Support was generously provided by the U.S. Army Natick RD&E Center (Contract No. DAAK60-91-K-005), the donors of the American Chemical Society Petroleum Research Fund (Grant 25218-AC), and the 3M Co.

References and Notes

(1) Tomasic, J.; Jennings, H. J.; Glaudemans, C. P. J. *Carbohydr. Res.* **1978**, *62*, 127.
(2) Han, Y. W. In *Advances in Applied Microbiology*; Neidleman, S. L., Laskin, A. I., Eds.; Academic Press: San Diego, 1990; Vol. 35; p 171.
(3) Keith, J.; Wiley, B.; Ball, D.; Arcidiacono, S.; Zorfass, D.; Mayer, J.; Kaplan, D. *Biotechnol. Bioeng.* **1991**, *38*, 557.
(4) Simms, P. J.; Boyko, W. J.; Edwards, J. R. *Carbohydr. Res.* **1990**, *208*, 193.
(5) Kaplan, D. L.; Mayer, J. M.; Ball, D.; McCassie, J.; Allen, A. L.; Stenhouse, P. In *Biodegradable Polymers and Packaging*; Ching, C., Kaplan, D. L., Thomas, E. L., Eds.; Technomic: Lancaster, PA, 1993; p 1.
(6) Cox, M. K. *Mol. Cryst. Liq. Cryst.* **1987**, *153*, 415.
(7) Ryan, T. G. *Mol. Cryst. Liq. Cryst.* **1988**, *157*, 577.
(8) Donald, A. M.; Windle, A. H. *Liquid Crystalline Polymers*, 1st ed.; Cambridge University Press: Cambridge, U.K., 1992.
(9) Viney, C.; Huber, A.; Verdugo, P. In *Biodegradable Polymers and Packaging*; Ching, C., Kaplan, D. L., Thomas, E. L., Eds.; Technomic: Lancaster, PA, 1993; p 209.
(10) Huber, A. E.; Stayton, P. S.; Viney, C.; Kaplan, D. L. *Macromolecules* **1994**, *27*, 953.
(11) Huber, A. E.; Kaplan, D. L.; Viney, C. *J. Environ. Polym. Degrad.* **1994**, *2*, 195.
(12) Huber, A. E. Ph.D. Dissertation, University of Washington, Seattle, WA, 1996. Copies available from University Microfilms, 1490 Eisenhower Place, P.O. Box 975, Ann Arbor, MI 48106.
(13) Mathews, C. K.; van Holde, K. E. *Biochemistry*; Benjamin/Cummings Publishing Co.: Redwood City, CA, 1990.
(14) Han, Y. W.; Clarke, M. A. *J. Agric. Food Chem.* **1990**, *38*, 393.
(15) Monomeric Cyanine Nucleic Acid Stains. Molecular Probes Report No. MP3602 06/23/94, Eugene, OR, 1994.
(16) Berne, B. J.; Pecora, R. *Dynamic Light Scattering*; John Wiley and Sons: New York, 1976.
(17) Wang, J.; Reitz, F.; Donaldson, T.; Pagliaro, L. *J. Biochem. Biophys. Methods* **1994**, *28*, 251.
(18) Zero, K.; Pecora, R. In *Dynamic Light Scattering: Applications of Photon Correlation Spectroscopy*; Pecora, R., Ed.; Plenum: New York, 1985; p 59.
(19) Twieg, R. J.; Chu, V.; Nguyen, C.; Dannels, C.; Viney, C. *Liq. Cryst.* **1996**, *20*, 287.
(20) Masing, G. *Ternary Systems*; Dover Publications: New York, 1960.
(21) Findlay, A. *The Phase Rule and its Applications*; Longmans, Green and Co.: London, 1927.
(22) Griffin, B. P.; Cox, M. K. *Br. Polym. J.* **1980**, *12*, 147.
(23) Northolt, M. G.; Sikkema, D. J. *Adv. Polym. Sci.* **1990/91**, *98*, 115.
(24) Stivala, S. S.; Bahary, W. S. *Carbohydr. Res.* **1978**, *67*, 17.
(25) French, A. D. *Carbohydr. Res.* **1988**, *176*, 17.
(26) Stryer, L. *Biochemistry*, 3rd ed.; W. H. Freeman and Company: New York, 1988.
(27) Merchant, K.; Rill, R. L. *Macromolecules* **1994**, *27*, 2365.
(28) Kerst, A.; Chmielewski, C.; Livesay, C.; Buxbaum, R. E.; Heidemann, S. R. *Proc. Natl. Acad. Sci. U.S.A.* **1990**, *87*, 4241.
(29) Suzuki, A.; Maeda, T.; Ito, T. *Biophys. J.* **1991**, *59*, 25.
(30) Hitt, A. L.; Cross, A. R.; Williams, R. C., Jr. *J. Biol. Chem.* **1990**, *265*, 1639.
(31) Perutz, M. F.; Liquori, A. M.; Eirich, F. *Nature* **1951**, *167*, 929.
(32) Viney, C.; Huber, A. E.; Dunaway, D. L.; Kerkam, K.; Case, S. T. In *Silk Polymers: Materials Science and Biotechnology*; Kaplan, D. L., Adams, W. W., Farmer, B. L., Viney, C., Eds.; American Chemical Society: Washington, DC, 1994; Vol. 544; p 120.
(33) Viney, C. *Supramol. Sci.* **1997**, *4*, 75.
(34) Flory, P. J. *J. Polym. Sci.* **1961**, *49*, 105.
(35) Flory, P. J. *Proc. R. Soc. London* **1956**, *A234*, 73.
(36) Bedford, S. E.; Yu, K.; Windle, A. H. *J. Chem. Soc., Faraday Trans.* **1992**, *88*, 1765.
(37) Flory, P. J.; Ronca, G. *Mol. Cryst. Liq. Cryst.* **1979**, *54*, 289.
(38) Flory, P. J. *Adv. Polym. Sci.* **1984**, *59*, 1.
(39) Weast, R. C., Ed. *CRC Handbook of Chemistry and Physics*, 64th ed.; CRC Press: Boca Raton, FL, 1983.

MA961705H